

Optimal Design for Flexible Passive Biped Walker Based on Chaotic Particle Swarm Optimization

Yao Wu*, Daojin Yao* and Xiaohui Xiao[†]

Abstract – Passive dynamic walking exhibits humanoid and energy efficient gaits. However, optimal design of passive walker at multi-variable level is not well studied yet. This paper presents a Chaotic Particle Swarm Optimization (CPSO) algorithm and applies it to the optimal design of flexible passive walker. Hip torsional stiffness and damping were incorporated into flexible biped walker, to imitate passive elastic mechanisms utilized in human locomotion. Hybrid dynamics were developed to model passive walking, and period-one gait was gained. The parameters global searching scopes were gained after investigating the influences of structural parameters on passive gait. CPSO were utilized to optimize the flexible passive walker. To improve the performance of PSO, multi-scroll Jerk chaotic system was used to generate pseudorandom sequences, and chaotic disturbance would be triggered if the swarm is trapped into local optimum. The effectiveness of CPSO is verified by comparisons with standard PSO and two typical chaotic PSO methods. Numerical simulations show that better fitness value of optimal design could be gained by CPSO presented. The proposed CPSO would be useful to design biped robot prototype.

Keywords: Biped robot, Chaos, Multi-variable optimal design, Passive dynamic walking, PSO.

1. Introduction

Stable and fast locomotion is one of mobile robots' primary tasks. Biped robots, inspired by human being, have received much attention in recent years due to their adaptability to work in complex environments [1, 2]. Many typical biped robots, such as ASIMO [3], HRP [4] and ATLAS [5] have advanced the development of humanoid robots. To implement stable bipedal locomotion, several biped robots are controlled under zero moment point (ZMP) method [6]. By precisely controlling joint angles, stable biped walking could be achieved if the ZMP is kept within the convex hull of the supporting area [7-9]. However, motions achieved by ZMP are inefficient and unnatural looking [10]. Another approach inspired by passive dynamic walking (PDW) could be utilized to produce humanoid and energy efficient biped gaits.

PDW is one locomotion manner where the robot walks down shallow slope without any actuation, powered only by gravity [11]. Passive walker fully employs the intrinsic dynamics of the robot, exhibiting an energy-efficient and humanlike walking gait. However, PDW is sensitive to initial conditions and disturbances. Quasi-passive walking, where active actuation was introduced for energy input and stabilization against large disturbance, has increased the versatility of PDW and gained successful application to level ground walking [12]. The study of PDW could

provide a deeper view of the human locomotion and inspire a more anthropomorphic biped prototype design.

Apart from actuation utilized to implement robust PDW gait, many efforts based on biomechanics have been made to design an anthropomorphic passive walker model, such as active leg compliance added in [13], and elastic passive joints used in [14]. Flexible passive walker is one kind of robot model where artificial compliance is introduced to the robot body. Experiments [15] showed that passive elastic mechanisms at the hip contribute substantially to normal human walking. Comparisons indicated that the torsional stiffness incorporated in the hip joint would be helpful to reduce the torque cost in bipedal locomotion, particularly at a high walking speed [16]. So humanoid and energy efficient walking gait can be achieved under a proper designed flexible passive biped model [17].

Since there are many structural parameters involved in the passive walker model, the model design problem is a typical multi-variable optimization task. Mass distribution, leg length, feet parameter and compliance are key variables in the flexible passive walker model. The mass distribution of passive biped walker was optimized in [18], and results showed that maximal robustness and highest walking speed are partly conflicting objectives of optimization. The effects of different foot shape (i.e. point-foot, round-foot and flat-foot) on passive gaits were investigated in [19]. However, most previous optimization works for passive walker put emphasis on single model variable. To the best of the authors' knowledge, multi-variable optimization of PDW model is rarely considered before.

Particle swarm optimization (PSO) is one multi-variable

[†] Corresponding Author: School of Power and Mechanical Engineering, Wuhan University, China. (xhxiao@whu.edu.cn)

* School of Power and Mechanical Engineering, Wuhan University, China. ({wuyao, ydaojin }@whu.edu.cn)

Received: August 9, 2017; Accepted: June 30, 2018

optimization method which could be utilized in the optimal design of passive biped dynamic walker task. Inspired by the observations of social animals, PSO has gained its successful applications in many fields, such as power systems [20], antenna design [21], and robotics [22]. The particles of PSO are placed in the search space of problem and evaluated by fitness function. By updating velocities and positions, particles move toward optimal solution to the problem. Significant benefits of PSO are the simplicity of implementation and fast convergence. However, PSO often suffers the problem of intrinsic premature (i.e. cause a particle to stagnate and may prematurely converge on suboptimal solutions that are not even guaranteed to be local optimum [23]). This paper proposes a Chaotic Particle Swarm Optimization (CPSO) algorithm, based on Chaos theory, to improve the performance of PSO.

Chaos can be described as a highly unstable motion of nonlinear deterministic systems in finite phase space [24]. Chaotic systems are highly sensitive to initial conditions, topologically mixing and dense in periodic orbits [25], which exhibit ergodicity, randomness and regularity. Many efforts have been made to combine PSO with chaotic systems, which could be mainly classified as two types [24]. In the first type, the chaotic sequences were used to tune the parameters of velocity update equation, such as the inertia weight w determined by Logistic chaotic map [26], and random numbers r_1 and r_2 replaced by chaotic numbers in [27]. In the second type, the chaotic search in particle space would be conducted when PSO was trapped into local optima, such as inactive particles were randomly generated and incorporated in the new population [28]. However, the dimensionality of chaotic system used in previous efforts, is lower than three. The low dimensional chaotic system, such as Logistic map and Tent Map, is easy to implement, but would be inefficient for high-dimensional optimization tasks. In this paper, a novel CPSO was proposed to improve the performance of PSO. The main difference between the presented CPSO and other chaos PSO methods could be concluded as: (1) multi-scroll Jerk chaotic system was used in this paper, rather than the low dimensional chaotic map. Three-dimensional chaotic sequences could be produced in one time, which showed good pseudo-randomness. (2) the original particle swarm was initialized by multi-scroll Jerk chaotic sequences, to improve the diversity of the swarm. (3) the variance of particles was evaluated. And chaotic disturbance would be triggered if the swarm is trapped into local optimum.

This paper aims to perform an optimal design of the flexible passive dynamic walker, after investigating the parameters' effects on PDW gait. The main contribution of this paper is proposing a novel CPSO algorithm based on chaos theory and applying it to the optimal design task of planar passive walker. A means for computing the swarm diversity is given and chaotic disturbance is proposed to improve PSO's performance in global search. Steady walking speed up to 1.8 m/s was found along optimized

structural parameters. The discussion could be useful to guide optimal design of the passive walker prototype.

The rest of the paper is organized as followed: section 2 builds up the mathematical model of the passive walking, based on hybrid dynamics. Typical period gait was found and parametric study was discussed in section 3. Section 4 conducts optimal design based on CPSO for passive walker. Conclusions are drawn in section 5.

2. Dynamics

In this section, a hybrid dynamics model for planar two-link passive biped walker was developed. All motions of planar biped are assumed to take place in the sagittal plane. There are two successive phases in one bipedal walking cycle: *swing phase* (SP) that only one leg contacts the ground, while *double support phase* (DSP) means that two legs touch the ground at the same time. During swing phase, the leg contacting the ground is named the *support leg* and the other is called the *swing leg*. Hybrid dynamics, based on the continuous dynamics for swing phase and algebraic equation for double support phase, could be used to describe the whole motion process of the PDW.

2.1 Swing phase

The proposed flexible passive dynamic walker is delineated as the Fig. 1. This model is composed of two identical rigid legs with round feet, linked with a frictionless hip joint. The mass of torso is concentrated as the hip mass m_h . To model passive mechanisms in human being, torsional spring stiffness k_{hip} and damping d_{hip} are incorporated in the hip. The mass distribution of leg is given by the leg mass m_l , moment of inertia J_l , the vertical position of the center of mass c , and the horizontal offset w_l . The passive walker travels downhill on a constant slope γ . To get general results, the parameters are normalized such that $m_l=1$, normalized time as $t/\sqrt{g/l}$. Structural parameters of the proposed model are listed as Table 1.

The generalized coordinate could be defined as

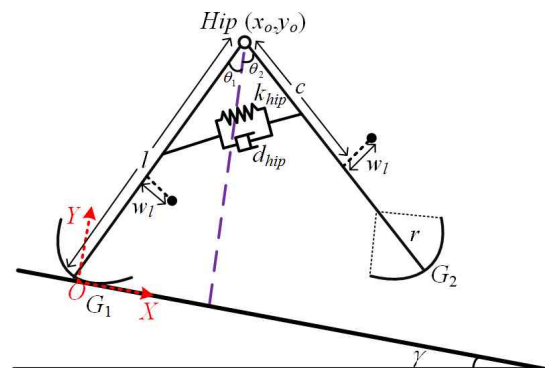


Fig. 1. Model of passive dynamic walker

Table 1. Structural parameters

Parameter	Meaning	Value
l	length of leg	0.5 m
m_l	mass of leg	1 kg
k_{hip}	torsional spring stiffness	0.95 N·m/rad
d_{hip}	damping of the hip	0.003 N·m·s/rad
γ	slope angle	0.02 rad
g	gravitational acceleration	9.8 m/s ²
k_c	$k_c=c/l$	0.2
k_r	$k_r=r/l$	0.4
k_j	$k_j=J_l/(ml^2)$	0.1592
k_w	$k_w=w_l/l$	-0.0005
β	$m_l=\beta m_1$	2

$$x = [q, \dot{q}]^T = [\theta_1, \theta_2, \dot{\theta}_1, \dot{\theta}_2]^T \quad (1)$$

where q is the position variable, and \dot{q} is the velocity variable. θ_1 is the angular position of the leg with respect to vertical of the support leg, and θ_2 is the angular position of the leg with respect to vertical of the swing leg. $\dot{\theta}_1, \dot{\theta}_2$ is the angular velocity respectively. As shown in the Fig. 1, OXY is the coordinate fixed on the slope, while Y-direction is vertical to the slope [29].

The continuous equation of swing phase motion based on Lagrange method then becomes

$$M(q)\ddot{q} + C(q, \dot{q})\dot{q} + G(q) = Q_f \quad (2)$$

where $M(q)$ is the inertia matrix, $C(q, \dot{q})$ is the matrix of Coriolis and centrifugal terms, $G(q)$ is the gradient of the potential energy, and Q_f describes the non-conservative forces on the generalized coordinates.

This dynamics equation in state space could be described as in (3).

$$\dot{x} = \begin{bmatrix} \dot{q} \\ M^{-1}(q)[Q_f - C(q, \dot{q})\dot{q} - G(q)] \end{bmatrix} = g(x) \quad (3)$$

2.2 Double support phase

The dynamic of double support phase could be described as a rigid and instantaneous impact model under premises [30]: (a) the impact takes place over an infinitesimally small period of time; (b) the external forces during the impact can be represented by impulses; (c) leg neither slips nor rebounds on the slope.

Due to the external forces could be regarded as impulses, the configuration of biped walker during DSP keeps the same. After impact, the role of swing leg and support leg is changed as in (4), where the superscript “+” (resp. “-”) refers to the value just after (resp. just prior to) the impact.

$$q^+ = Jq^-, \quad J = \begin{bmatrix} 0 & 1 \\ 1 & 0 \end{bmatrix} \quad (4)$$

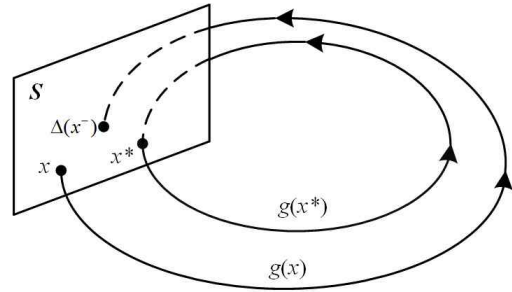


Fig. 2. Hybrid dynamics

The angular velocities after impact could be derived under conservation of angular momentum law. Specifically, the conservation of angular momentum of the whole system to the contact point, and the conservation of angular momentum of the support leg to the hip connection, which could be derived as in (5).

$$Q^-(q)\dot{q}^- = Q^+(q)\dot{q}^+ \quad (5)$$

Denote $R(q) = (Q^+(q))^{-1}Q^-(q)$, and the status after double support phase is derived as

$$x^+ = \begin{bmatrix} q^+ \\ \dot{q}^+ \end{bmatrix} = \begin{bmatrix} J & 0 \\ 0 & R(q) \end{bmatrix} \begin{bmatrix} q^- \\ \dot{q}^- \end{bmatrix} = \Delta(x^-) \quad (6)$$

So one algebraic Eq. (6) could be used to describe the DSP model. The leg-ground impact happens when the swing leg contacts the ground, and the impact condition could be derived from geometry as in (7) for symmetric legs. For simplicity, the foot-scuffing is neglected in simulation.

$$S: \theta_1^- + \theta_2^- = 0 \quad (7)$$

2.3 Hybrid dynamics

The hybrid dynamics for the flexible two-link passive biped walker could be derived by combining continuous dynamic Eq. (3) and impact Eq. (6). The hybrid dynamics written in state-space form are as in (8).

$$\begin{cases} \dot{x} = g(x), & x^- \notin S \\ x^+ = \Delta(x^-), & x^- \in S \end{cases} \quad (8)$$

The calculation process of the hybrid dynamics could be delineated as Fig. 2. Starting from the initial value as $x=x_0$, the continuous Eq. (3) could be calculated until the impact (7) happened. The next status x_0^+ after DSP could be derived as (6). Then continuous Eq. (3) could proceed with $x=x_0^+$. If there is one fixed-point x^* , the status after one cycle would be x^* , and period gait could be gained.

3. Parametric Study

3.1 Typical gait and stability analysis

Under appropriate structural parameters and initial value x_0 , successful PDW gait could be gained. Period-one gait in passive walking corresponds to the fixed-point x^* of PDW trajectory, which could be derived by Cell Mapping method [31]. Cell Mapping method discretizes a region of the state space into cells. The dynamics output starting from each cell is defined as image cell. By analyzing the resulting graph of the cell space, fixed points and basin of attraction could be found [32].

As for the passive walker shown as Fig. 1, the original value x_0 calculated by Cell Mapping method to implement a period-one locomotion is $[0.3285, -0.3285, -1.4206, -1.2684]^T$. The PDW gait starting from x_0 under structural parameters as Table 1, is depicted as Fig. 3. From Fig. 3, it could be seen single period one passive gait could be got. The periodicity of gait shows the success of passive dynamic walking.

To evaluate the stability of the PDW gait, maximum Floquet multiplier was utilized, which quantifies how the system's states respond to local perturbations discretely from one cycle to the next at a single point during the cycle [33]. As shown in the Fig. 2, consider a point x in S and a trajectory emanating from it. This trajectory may or may not intersect S . If it does, let the point of intersection be denoted by x^+ . With regard to the hybrid dynamics of passive biped, the impact of DSP could be used as the Poincaré section [34], and the status after DSP is x^+ as in (6).

The resulting Poincaré map P could be defined as $P: x \rightarrow x^+$. The motions starting from state x_i could be derived as $x^{i+1} = P(x^i)$ where P stands for Poincaré map.

Let assume there exists one fixed-point as $x^* = P(x^*)$ and there is small disturbance at x^* , i.e. $x^i = x^* + \Delta x^i$. Then partial linearization of the Poincaré map could be derived as

$$x^{i+1} = P(x^i) = P(x^* + \Delta x^i) \approx P(x^*) + J(x^*)\Delta x^i \quad (9)$$

where $J(x^*)$ stands for Jacobian matrix at fixed-point x^* , i.e.

$$J(x^*) = \begin{bmatrix} \frac{\partial P_1(x^*)}{\partial x_1} & \dots & \frac{\partial P_1(x^*)}{\partial x_n} \\ \vdots & \dots & \vdots \\ \frac{\partial P_n(x^*)}{\partial x_1} & \dots & \frac{\partial P_n(x^*)}{\partial x_n} \end{bmatrix} \quad (10)$$

So

$$\Delta x^{i+1} = x^{i+1} - x^* = J(x^*)\Delta x^i \quad (11)$$

If the maximal modulus of eigenvalues λ_{max} of $J(x^*)$ is small than one, then an exponentially stable fixed point could be gained [34]. In short, maximum Floquet multiplier could be derived as the maximal modulus of eigenvalue λ_{max} in Jacobian matrix of Poincaré map.

However, due to the hybrid property of biped dynamics, it is difficult to get the closed-form of biped's Poincaré map function and Jacobian matrix. The numerical approximation of Jacobian matrix could be utilized as [35]:

$$J(x^*) = \begin{bmatrix} \frac{P(x^* + dx_1) - P(x^*)}{dx_1}, \frac{P(x^* + dx_2) - P(x^*)}{dx_2}, \dots, \\ \frac{P(x^* + dx_n) - P(x^*)}{dx_n} \end{bmatrix} \quad (12)$$

where $dx_1 = [dx, 0, \dots, 0]^T$, $dx_2 = [0, dx, \dots, 0]^T$, ..., $dx_n = [0, \dots, dx]^T$. Every column of the Jacobian matrix is gained by calculating the Poincaré map $P(x^* + dx_i)$ starting from the disturbed original value $x^* + dx_i$ ($i=1, 2, \dots, n$).

To evaluate the stability of the PDW gait starting from original value $x_0 = [0.3285, -0.3285, -1.4206, -1.2684]^T$ under disturbance $dx=10^{-6}$, the modulus of eigenvalue of the Jacobian matrix are calculated as $[0.7969, 0.6316, 0.0136]$. Since the maximum Floquet multiplier ($\lambda_{max} = 0.7969$) is smaller than 1, the gait is stable under small disturbance. It is noted that λ_{max} is used as a stability descriptor for fitness function in optimal design in section 4.

3.2 Influences of structural parameters

To provide a global search scope for optimal design, the influences of structural parameters on PDW gaits were investigated. To be specific, the single variable method (i.e. only one factor is changed from trial to trial [36]) is used to evaluate parameters' effects on passive gait and provide a suitable global searching zone for stable PDW. Three gait descriptors were used in this paper to judge walking gait: step length L_s defined as the tangential distance between the positions where swing leg leaves the ground and touches the ground in one walking cycle as shown in the

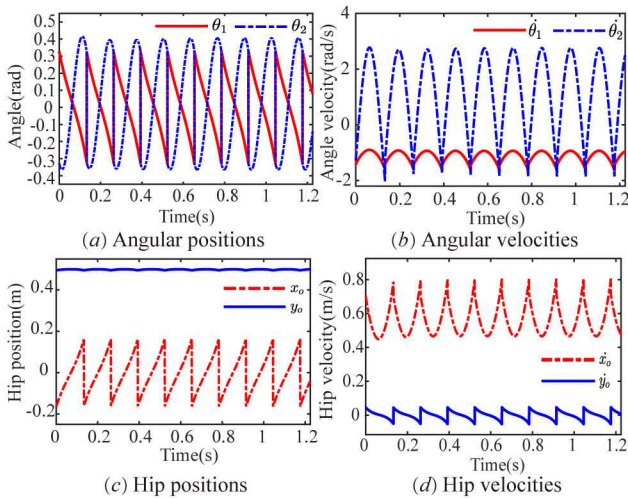


Fig. 3. Typical single period gait

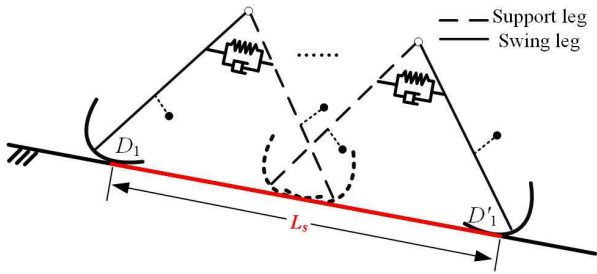


Fig. 4. Step length L_s

Table 2. The effects of structural parameters

Parameter	Scope	Step length	Step period	Step velocity
$\beta \uparrow$	[1, 6.5]	\uparrow	invariant	\uparrow
$k_{hip} \uparrow$	[0.91, 1.13]	\downarrow	\downarrow	\uparrow
$d_{hip} \uparrow$	[0, 0.007]	\downarrow	\downarrow	\uparrow
$k_j \uparrow$	[0.08, 0.26]	\uparrow	\uparrow	\downarrow
$k_c \uparrow$	[0.1, 0.65]	\downarrow to constant	\downarrow then \uparrow	\uparrow then \downarrow
$k_w \uparrow$	[-0.007, 0.003]	\uparrow then \downarrow	\downarrow	\uparrow
$k_r \uparrow$	[0.40, 0.76]	\uparrow	\downarrow	\uparrow

Fig. 4, step period P_s defined as the duration from swing leg end leaves the ground to the moment swing leg contacts the ground, and step velocity v_{step} defined as

$$v_{step} = \frac{L_s}{P_s} \quad (13)$$

The structural parameters of the proposed model include hip stiffness k_{hip} and damping d_{hip} . Other parameters were all nondimensionalized based on leg mass m_l and leg length l as hip mass $\beta = m_h/m_l$, moment of inertia $k_j = J_l/m_l l^2$, horizon mass offset $k_w = w_l/l$, vertical position $k_c = c/l$, and radius of round feet $k_r = r/l$. Three descriptors are all steady value of passive walking under origin value $x_0 = [0.3285, -0.3285, -1.4206, -1.2684]^T$. This paper takes interest in stable passive walking, so the unstable parameter zone was not considered.

The influence of structural parameters on PDW gaits was summarized as Table 2. As Table 2 shows, the structural parameters have different influences on PDW gait. Besides, the couple of parameters results in a complex effect on passive gait. The parametric study could be used to provide global search scopes for optimal PDW model design. Since there are seven structural parameters, the optimal design of passive walker is a typical multi-variable optimization task.

4. Optimal Design based on CPSO

4.1 Overview of CPSO

A systematic numerical exploration of the multi-dimensional parameter space is necessary to perform an optimal design for passive walker. As a population-base,

self-adaptive global search optimization technique, PSO is suitable for multi-variable optimization tasks. The swarm in PSO is a group of particles, where each particle has its position, velocity and fitness value. The position of particle stands for the possible solution to the optimization problem, which is updated based on velocity. The determination of particle's velocity is based on particle's ability to maintain its old velocity, experience learned from its history and experience from the swarm's history. In general, PSO could perform a good search based on exploration of the solution space and exploitation of its best history.

Specifically, the velocity of particles $v(i,k)$ is defined as (14). The particles' velocity update law consists of three parts: inertial parameter w which provides the necessary momentum for particles to roam across the search space; self-learning parameter c_1 describing particle's ability to learn from its own experience, which encourages the particle to move toward its own best position p_{best} ; social-learning parameter c_2 describing the ability to learn from experience of the swarm, which pulls the particles toward the global group best particle g_{best} found so far [37].

$$v^{t+1}(i,k) = wv^t(i,k) + c_1 \times r_1 \times [p_{best}^t(i,k) - x^t(i,k)] + c_2 \times r_2 \times [g_{best}^t(i,k) - x^t(i,k)] \quad (14)$$

where t stands for the iteration number, i means the i^{th} particle, and k stands for the k^{th} dimension of the particle. r_1 and r_2 are two uniformly distributed random numbers in the range [0,1] which were separately generated.

Position of particle $x(i,k)$ is updated according to (15).

$$x^{t+1}(i,k) = x^t(i,k) + v^t(i,k) \quad (15)$$

The component of $v(i,k)$ and $x(i,k)$ was clamped to the range $[-V_{max}, V_{max}]$ and $[-X_{max}, X_{max}]$ respectively, to control excessive roaming of particles outside the search space.

In this paper, an optimal design for planar flexible passive dynamic walker is conducted based on PSO. Since there is no energy compensated into passive walker, the energy cost of transport (i.e. energy per unit distance, per unit body weight) for passive walker on a given slope γ is $\sin\gamma$ [19], which is not related to structural parameters. So the energy cost of transport is not used as fitness function. Since the flexible biped robot was developed to implement humanoid locomotion, stable fast walking was utilized as the target of optimization.

Let f stand for fitness function. The particle best position p_{best} and group best position g_{best} could be described as

$$p_{best}^{t+1}(i,k) = \begin{cases} p_{best}^t(i,k), & f(x(i,k)) \leq f(p_{best}^t(i,k)) \\ x(i,k), & f(x(i,k)) > f(p_{best}^t(i,k)) \end{cases} \quad (16)$$

$$g_{best}^{t+1}(i,k) = \arg \max_x [f(x(i,k)), f(g_{best}^t(i,k))] \quad (17)$$

where initial values at $t=0$ were set as $p_{best}=0, g_{best}=0$.

There are benefits of PSO in global optimization tasks, such as simplicity of implementation and rapid convergence

rate. However, the standard PSO (SPSO) suffers from its premature problem, where particles loss their diversity and fail to get rid of local optima situation. To improve the performance of SPSO, a chaotic PSO (CPSO) algorithm is proposed in this paper. The key points of the proposed CPSO could be concluded as: (1) multi-scroll Jerk chaotic system was used to generate pseudorandom sequences. (2) the inertial parameter was adjusted in a non-linear way to balance the exploration ability and exploitation ability. (3) swarm variance was utilized to describe the diversity of the particle swarm. Chaotic disturbance was used to make the particles to jump out of the local optima.

4.2 Multi-scroll Jerk chaotic system

Low dimensional chaotic system, such as Logistic map, was used to generate pseudorandom numbers in previous CPSO efforts [24]. However, low dimensional chaotic systems could be inefficient for multi-variable optimization task, to produce multi-dimensional random numbers. Jerk chaotic system was used in this paper, to produce three-dimensional pseudorandom sequences in one time.

It is worth noting that Jerk chaotic map exhibits a multi-scroll shape in state space [38]. With the increase of scrolls, improvement of diversity could be gained in multi-scroll chaotic systems [39].

The Euler discretization equation of multi-scroll Jerk chaos [39] is utilized as followed.

$$\begin{cases} x(n+1) = x(n) + y(n) \cdot T \\ y(n+1) = y(n) + z(n) \cdot T \\ z(n+1) = z(n) + [-x(n) - y(n) - \alpha z(n) + F(x(n))] \cdot T \end{cases} \quad (18)$$

where x, y, z is the pseudorandom sequence produced by Jerk chaotic system. T is the period. The nonlinear function $F(x)$ is described as (19), and $\alpha=0.55$.

$$F(x) = A \operatorname{sgn}(x(n)) + A \sum_{p=1}^N \operatorname{sgn}(x(n) - 2pA) + A \sum_{q=1}^N \operatorname{sgn}(x(n) + 2qA) \quad (19)$$

where p, q was variable to control the scroll numbers in state space. For instance, N was set to 3 to produce eight-scroll chaotic sequences, $A=0.5, x(0)=0.02, y(0)=0.01, z(0)=0.12$.

Fig. 5(a) shows the sequence y produced by eight-scroll Jerk dynamic system. From Fig. 5(a), y sequence is randomly changed, which shows the pseudo-randomness and ergodicity of chaos. The state-phase picture of (x, y) sequences is depicted as Fig. 5(b). It could be seen that the (x, y) states form eight scrolls, and randomly change in the state space, which shows an element of regularity.

The pseudorandom sequences produced by Jerk chaotic system was used to initiate positions and velocities of the original swarm. Furthermore, the chaotic disturbance in

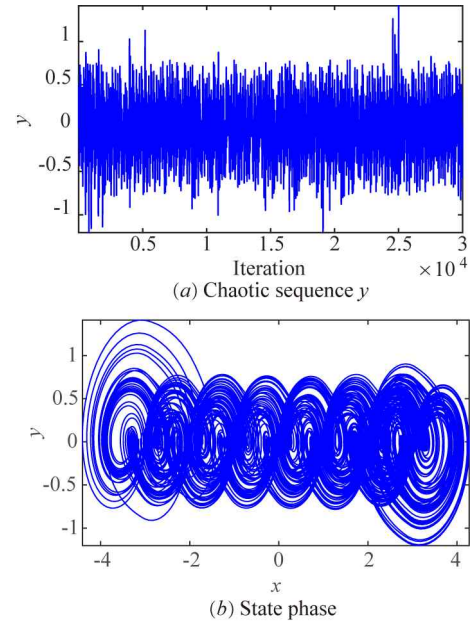


Fig. 5. The eight-scroll Jerk Chaotic system

section 4.4 was also based on Jerk chaotic map.

4.3 Adjustment of inertial parameter

Proper control of exploration and exploitation ability of PSO is crucial in successfully finding the optimum solution. Inertial parameter w is used to balance the ability of global search and local search, since a large w is more appropriate for exploration (i.e. global search) while a small w facilitates exploitation (i.e. local search).

Inertial weight is adjusted in this paper in a non-linear way to balance the local and global search as in (20). In the beginning of iterations, the larger w means that particles would have higher tendency to maintain its former velocity, leading to improve swarm's exploration ability to the whole possible solution space. In the later process, w decreased to smaller values, making precise local search. The balance of global searching and local searching would be helpful to improve the PSO's overall searching ability.

$$w_i = (w_{start} - w_{end}) \cdot \left(\frac{t_i}{t_{max}} \right)^2 - (w_{start} - w_{end}) \cdot \frac{2t_i}{t_{max}} + w_{start} \quad (20)$$

where t_{max} is the maximal iteration number, w_{start} is the beginning value of w for global searching and w_{end} is the end value for local searching.

4.4 Chaotic disturbance

One feature of PSO is that particles almost all keep the same in the later period of iteration. If the swarm is stuck in local optimal, it is difficult to jump out of it. Swarm variance was used to describe the diversity of the particle swarm as in (21).

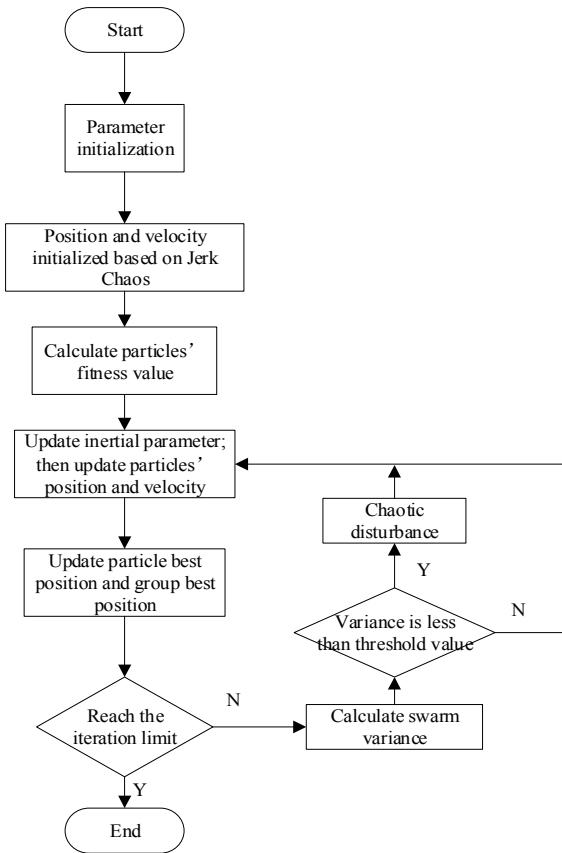


Fig. 6. Flow chart of CPSO

$$\sigma^2 = \sum_{i=1}^N (f_i - \bar{f})^2 \tag{21}$$

where \bar{f} is the mean fitness value of the present swarm. If swarm variance was below the threshold value, chaotic disturbance would be triggered to make the swarm jump out of the local optima. The threshold value was manually set by trial-and-error experience. The pseudocode for chaotic disturbance is describe as Algorithm 1. The flowchart of the CPSO is delineated as Fig. 6. Specifically, the swarm variance is evaluated as in (21) during iteration, and the chaotic disturbance is triggered if swarm is trapped in local optimal. The global fitness value is used to produce Jerk chaotic sequences, which were used to replace the previous particles.

Algorithm 1. Framework of chaotic disturbance.

Input: The global best position g_{best}

Output: The disturbed particles

1. normalize the global fitness value $f(g_{best})$ to disturbance origin value $n_r \in [0,1]$;
2. chaos series M produced by the multi-scroll Jerk system with origin value $x(0) = n_r$;
3. transfer M series back to variable zone, and calculate the corresponding fitness value;
4. **return** maximum of fitness particles to the swarm

4.5 Results

The optimal design of flexible passive dynamic walker is a multi-variable parameters optimization problem, which could be described as

$$\begin{aligned} \max \quad & f = flag \cdot (a_1 \cdot v_{step} + a_2 \cdot \frac{1}{\lambda_{max}}) \\ \text{s.t.} \quad & 0.08 \leq k_j \leq 0.26, \quad -0.0070 \leq k_w \leq 0.0030 \\ & 1 \leq \beta \leq 6.5, \quad 0.910 \leq k_{hip} \leq 1.130 \\ & 0 \leq d_{hip} \leq 0.007, \quad 0.1 \leq k_c \leq 0.65 \\ & 0.4 \leq k_r \leq 0.76 \end{aligned} \tag{22}$$

There are seven structural parameters as variables in the optimal design of planar passive dynamic walker. To get more general results, structural parameters are normalized. The searching scope is derived from the stable walking zone listed in Table 2.

To implement a fast and stable bipedal locomotion, stable step velocity was used in fitness function f . There are three parts in fitness function to describe the maximal stable velocity. To be specific, $flag$ is used to mark the stable status. If biped walker failed, the $flag$ is set to zero. The $flag$ is set to one if stable walking could be achieved. v_{step} is the step velocity. λ_{max} is the maximum Floquet multiplier, standing for the stability. The walker is more stable if λ_{max} is smaller [40]. a_1 and a_2 are cost weights to trade-off proportion of velocity and stability in fitness value.

Optimal design for planar flexible passive walker was conducted based on CPSO. Specifically, the population size of CPSO is 50, and the dimension of each particle is 7. Inertial parameter w is adjusted as in (20) with $w_{start}=0.9$, $w_{end}=0.4$. The largest iteration number is set as 50. The cost weights in fitness function are $a_1=5$ and $a_2=5$.

To evaluate the performance of CPSO proposed in this paper, comparisons with standard PSO (SPSO) and two other chaotic CPSO methods are conducted. Random numbers r_1 and r_2 were replaced by chaotic sequences in CPSO1 [27]. And chaotic search is conducted as inactive particles were randomly generated and incorporated in the new population in CPSO2 [28]. The comparisons are delineated as Fig. 7.

As shown in Fig. 7(a), group best fitness value $f(g_{best})$ increased with the growth of iteration in four PSO methods. The fitness value of CPSO is obviously higher than the fitness value of SPSO. Besides, the result of CPSO this paper presented is higher than CPSO1 and CPSO2, which implies that better optimization results gained by the CPSO proposed. The superiority could be attributed to the features of the proposed CPSO: nonlinear adjustment of the inertial parameter, which balances the exploration and exploitation ability, and the chaotic disturbance to make the swarm jump out of local optima.

Fig. 7(b) shows the swarm variance of four PSO methods. It could be seen that the swarm variances of other

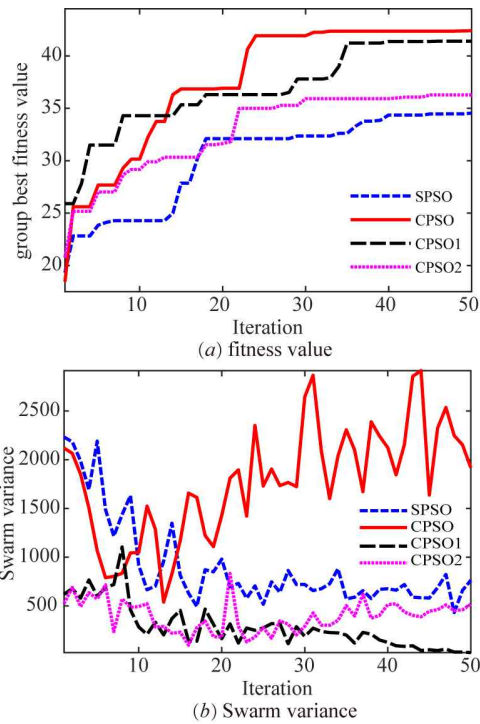


Fig. 7. The iteration results of CPSO and SPSO

PSO methods are low in the later iteration period, while particles of CPSO gained the highest swarm variance, which indicates high diversity of CPSO swarm. The swarm diversity of CPSO algorithm could be maintained, for the chaotic disturbance would be triggered if the swarm variance was below the threshold value, to improve the diversity of the swarm, while the other PSO algorithms would be trapped with the local optima and the swarm lost its diversity. The optimized structural parameters gained by CPSO are $[k_j, k_w, \beta, k_{hip}, d_{hip}, k_c, k_r] = [0.1527, -0.0042, 6.4030, 1.0880, 0.0024, 0.5004, 0.4000]$.

The weights in fitness function are useful to adjust the proportion of step velocity and stability in fitness function. Since the maximal robustness and highest walking speed are partly conflicting objectives of optimization [18], the fitness function (22) consists of two parts: velocity and stability, where weights parameters a_1 and a_2 were utilized to trade-off the proportions. For instance, to get higher velocity, the weight a_1 was set to 8 and a_2 was set to 3, making the velocity a larger proportion in fitness value. The optimized structural parameters gained by CPSO are $[k_j, k_w, \beta, k_{hip}, d_{hip}, k_c, k_r] = [0.0809, -0.0010, 6.4940, 0.9550, 0, 0.1000, 0.6289]$. The walking velocities by CPSO and PSO are delineated as Fig. 8. From Fig. 8, it could be seen that the PDW velocities under PSO methods are higher than the origin parameters in Table 1, while the velocity of CPSO optimization is higher than the result of SPSO. The passive gaits are found by CPSO, in which the stable velocity is up to 1.8 m/s.

The parameter a_2 marks proportion of stability in fitness function. For instance, the corresponding limit cycle

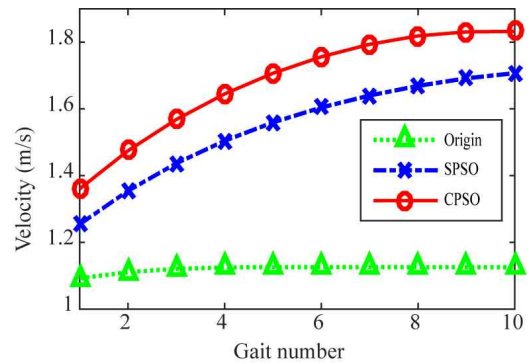


Fig. 8. The velocity results

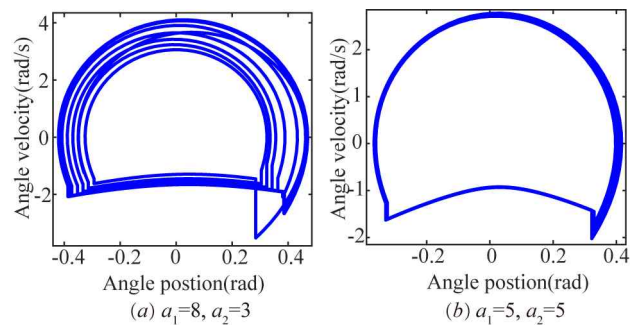


Fig. 9. The limit cycles

formed in state space of PDW gait is delineated as Fig. 9(a), under the structural parameters gained by CPSO ($a_1=8$ and $a_2=3$) $[k_j, k_w, \beta, k_{hip}, d_{hip}, k_c, k_r] = [0.0809, -0.0010, 6.4940, 0.9550, 0, 0.1000, 0.6289]$. Since there are some adjust gaits, the limit cycle may converge to the steady cycle after adjustment cycles, which implies the velocity of PDW could be increased at the cost of stability. Fig. 9(b) shows the limit cycle of gaits under parameters as $[k_j, k_w, \beta, k_{hip}, d_{hip}, k_c, k_r] = [0.1527, -0.0042, 6.4030, 1.0880, 0.0024, 0.5004, 0.4000]$, which were gained under balanced cost weights ($a_1=5$ and $a_2=5$) in CPSO. Due to there are few adjustment gaits, the limit cycle in Fig. 9(b) implies that period-one PDW gait would be gained.

5. Conclusion

This paper presented a Chaotic Particle Swarm Optimization (CPSO) algorithm and applied it to the optimal design of the flexible passive dynamic biped walker. First, the hybrid dynamics were built for flexible passive walker, in which the hip torsional stiffness and damping were introduced to imitate the elastic mechanisms in human being. Then the typical period passive gait was discussed. Parametric study was conducted to investigate the effects of structural parameters on PDW gaits and provide the global search scope for the multi-variable optimal model design. To improve PSO's performance and avoid the premature problem, CPSO was proposed.

The benefits of CPSO proposed in this paper could be concluded as: (1) three-dimensional chaotic sequences could be produced in one time, and the multi-scroll Jerk chaotic system was introduced to improve the diversity of the original swarm. (2) chaotic disturbance was employed to make the particle swarm escape from the local optimal. Optimal design based on CPSO for flexible passive dynamic walker was conducted, in terms of maximizing stable walking velocity. Effectiveness of the proposed CPSO algorithm has been demonstrated through comparisons with SPSO and other two typical Chaotic PSO, where the fitness values of CPSO are higher than the fitness values of other methods. Walking speeds up to 1.8 m/s are found via increasing the velocity weight a_1 in fitness function, at the cost of stability. The proposed method would be useful for the optimal prototype design of humanoid robots such as PDW walker.

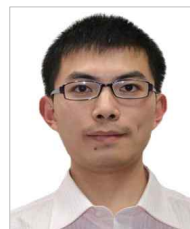
Acknowledgements

This research was supported by National Natural Science Foundation of China (NSFC, Grant No. 51675385 and 51175383). Part of numerical calculations in this paper have been done on the supercomputing system in the Supercomputing Center of Wuhan University.

References

- [1] Hayder FN Al-Shuka, Burkhard Corves, Wen-Hong Zhu, and Bram Vanderborght, "Multi-level control of zero-moment point-based humanoid biped robots: a review," *Robotica*, vol. 34, no. 11, pp. 2440-2466, 2016.
- [2] Bum-Joo Lee and Kab Il Kim, "Modifiable walking pattern generation handling infeasible navigational commands for humanoid robots," *Journal of Electrical Engineering & Technology*, vol. 9, no. 1, pp. 344-351, 2014.
- [3] Yoshiaki Sakagami, Ryujin Watanabe, Chiaki Aoyama, Shinichi Matsunaga, Nobuo Higaki, and Kikuo Fujimura, "The intelligent asimo: System overview and integration," *In Intelligent Robots and Systems, 2002. IEEE/RSJ International Conference on*, pp. 2478-2483, 2002.
- [4] Kenji Kaneko, Kensuke Harada, Fumio Kanehiro, Go Miyamori, and Kazuhiko Akachi, "Humanoid robot hrp-3," *In Intelligent Robots and Systems, 2008. IROS 2008. IEEE/RSJ International Conference on*, pp. 2471-2478, 2008.
- [5] Scott Kuindersma, Robin Deits, Maurice Fallon, Andrés Valenzuela, Hongkai Dai, Frank Permenter, Twan Koolen, Pat Marion, and Russ Tedrake, "Optimization-based locomotion planning, estimation, and control design for the atlas humanoid robot," *Autonomous Robots*, vol. 40, no. 3, pp. 429-455, 2016.
- [6] Miomir Vukobratovic and J Stepanenko, "On the stability of anthropomorphic systems," *Mathematical biosciences*, vol. 15, no. 1-2, pp. 1-37, 1972.
- [7] Hong, Young-Dae, Ki-Baek Lee, and Bumjoo Lee, "Dynamic simulation of modifiable walking pattern generation to handle infeasible navigational commands for humanoid robots," *Journal of Electrical Engineering & Technology*, vol. 11, no. 3, pp. 1921-1928, 2016.
- [8] Seungchul Lim and Young Ik Son, "Discrete-time circular walking pattern for biped robots," *Journal of Electrical Engineering & Technology*, vol. 11, no. 5, pp. 1395-1403, 2016.
- [9] Woong-Ki Lee, Dongkyoung Chwa, and Young-Dae Hong, "Control strategy for modifiable bipedal walking on unknown uneven terrain," *Journal of Electrical Engineering & Technology*, vol. 11, no. 6, pp. 1787-1792, 2016.
- [10] Ian R Manchester, Uwe Mettin, Fumiya Iida, and Russ Tedrake, "Stable dynamic walking over uneven terrain," *The International Journal of Robotics Research*, vol. 30, no. 3, pp. 265-279, 2011.
- [11] McGeer Tad, "Passive Dynamic Walking," *The International Journal of Robotics Research*, vol. 9, no. 2, pp. 62-82, 1990.
- [12] Fumihiko Asano, Masaki Yamakita, and Katsuhisa Furuta, "Virtual passive dynamic walking and energy-based control laws," *In Intelligent Robots and Systems, 2000. (IROS 2000). Proceedings. 2000 IEEE/RSJ International Conference on*, pp. 1149-1154, 2000.
- [13] Richard Quint Van Der Linde, "Active leg compliance for passive walking," *In Robotics and Automation, 1998, Proceedings, IEEE International Conference on*, pp. 2339-2344, 1998.
- [14] Fumiya Iida, Yohei Minekawa, Jürgen Rummel, and André Seyfarth, "Toward a human-like biped robot with compliant legs," *Robotics and Autonomous Systems*, vol. 57, no. 2, pp. 139-144, 2009.
- [15] Ben Whittington, Amy Silder, Bryan Heiderscheit, and Darryl G Thelen, "The contribution of passive-elastic mechanisms to lower extremity joint kinetics during human walking," *Gait & posture*, vol. 27, no. 4, pp. 628-634, 2008.
- [16] Narukawa, Terumasa, Masaki Takahashi, and Kazuo Yoshida. "Efficient walking with optimization for a planar biped walker with a torso by hip actuators and springs," *Robotica*, vol. 29, no. 4, pp. 641-648, 2011.
- [17] Wu, Yao, Daojin Yao, and Xiaohui Xiao, "The effects of ground compliance on flexible planar passive biped dynamic walking," *Journal of Mechanical Science and Technology*, vol. 32, no. 4, pp. 1793-1804, 2018.
- [18] Joachim Hass, J Michael Herrmann, and Theo Geisel, "Optimal mass distribution for passivity-based bipedal robots," *The International Journal of Robotics*

- Research*, vol. 25, no. 11, pp. 1087-1098, 2006.
- [19] Maxine Kwan and Mont Hubbard, "Optimal foot shape for a passive dynamic biped," *Journal of theoretical biology*, vol. 248, no. 2, pp. 331-339, 2007.
- [20] S. Anbarasi, and S. Muralidharan, "Hybrid bfpso approach for effective tuning of pid controller for load frequency control application in an interconnected power system," *Journal of Electrical Engineering & Technology*, vol. 12, no. 3, pp. 1027-1037, 2017.
- [21] Seong-In Kang, Koon-Tae Kim, Seung-Jae Lee, Jeong-Phill Kim, Kyung Choi, and Hyeong-Seok Kim, "A study on a gain-enhanced antenna for energy harvesting using adaptive particle swarm optimization," *Journal of Electrical Engineering & Technology*, vol. 10, no. 4, pp. 1780-1785, 2015.
- [22] Riccardo Poli, James Kennedy, and Tim Blackwell, "Particle swarm optimization," *Swarm intelligence*, vol. 1, no. 1, pp. 33-57, 2007.
- [23] Premalatha Kandasamy and A M Natarajan. "Combined Heuristic Optimization Techniques for Global Minimization," *International Journal of Advances in Soft Computing and Its Applications*, vol. 2, no. 1, pp. 85-99, 2010.
- [24] Yang Dixiong, Zhenjun Liu and Ping Yi. "Computational efficiency of accelerated particle swarm optimization combined with different chaotic maps for global optimization," *Neural Computing and Applications*, vol. 28, no. 1, pp. 1245-1264, 2017.
- [25] Yan Danping, et al. "Empirically characteristic analysis of chaotic PID controlling particle swarm optimization," *PloS one*, vol. 12, no. 5, pp. e0176359, 2017.
- [26] Chuang Li-Yeh, Cheng-Hong Yang, and Jung-Chike Li. "Chaotic maps based on binary particle swarm optimization for feature selection," *Applied Soft Computing*, vol. 11, no. 1, pp. 239-248, 2011.
- [27] Cheng-Hong Yang, Sheng-Wei Tsai, Li-Yeh Chuang and Cheng-Huei Yang. "An improved particle swarm optimization with double-bottom chaotic maps for numerical optimization," *Applied Mathematics and Computation*, vol. 219, no. 1, pp. 260-279, 2012.
- [28] Hong-ji Meng, Peng Zheng, Rong-Yang Wu, Xiao-Jing Hao and Zhi Xie. "A hybrid particle swarm algorithm with embedded chaotic search," *Cybernetics and Intelligent Systems, 2004 IEEE Conference on*, pp. 367-371, 2004.
- [29] Liu Ning, Li Junfeng, and Wang Tianshu, "The effects of parameter variation on the gaits of passive walking models: simulations and experiments," *Robotica*, vol. 27, no. 4, pp. 511-528, 2009.
- [30] Westervelt E R, Grizzle J W, Chevallereau C, et al. Feedback control of dynamic bipedal robot locomotion. CRC press, 2007.
- [31] C. S. Hsu, Cell to Cell Mapping A Method of Global Analysis for Nonlinear Systems. Springer Science+ Business Media, 1987.
- [32] Gyebrószki, Gergely, and Gábor Csernák. "Clustered Simple Cell Mapping: An extension to the Simple Cell Mapping method," *Communications in Non-linear Science and Numerical Simulation*, vol. 42, pp. 607-622, 2017.
- [33] Jonathan B Dingwell, Hyun Gu Kang, and Laura C Marin, "The effects of sensory loss and walking speed on the orbital dynamic stability of human walking," *Journal of biomechanics*, vol. 40, no. 8, pp. 1723-1730, 2007.
- [34] B. Morris and J. W. Grizzle, "A restricted poincare map for determining exponentially stable periodic orbits in systems with impulse effects: Application to bipedal robots," *In IEEE Conference on Decision and Control*, pp. 4199-4206, 2006.
- [35] Jie Zhao, Xiaoguang Wu, Xizhe Zang, et al, "The analysis on period doubling gait and chaotic gait of the compass-gait biped model," *In Robotics and Automation, 2011 IEEE International Conference on*, pp. 2015-2020, 2011.
- [36] Daniel D Frey and Hungjen Wang, "Adaptive one-factor-at-a-time experimentation and expected value of improvement," *Technometrics*, vol. 48, no. 3, pp. 418-431, 2006.
- [37] Asanga Ratnaweera, Saman K Halgamuge, and Harry C Watson, "Self-organizing hierarchical particle swarm optimizer with time-varying acceleration coefficients," *IEEE Transactions on evolutionary computation*, vol. 8, no. 3, pp. 240-255, 2004.
- [38] Chunhua Wang, Xiaoming Liu, and Hu Xia, "Multi-piecewise quadratic nonlinearity memristor and its 2n-scroll and 2n+1-scroll chaotic attractors system," *Chaos: An Interdisciplinary Journal of Nonlinear Science*, vol. 27, no. 3, pp. 033114, 2017.
- [39] Simin Yu, Jinhua Lu, Henry Leung, and Guanrong Chen, "Design and implementation of n-scroll chaotic attractors from a general jerk circuit," *IEEE Transactions on Circuits and Systems I: Regular Papers*, vol. 52, no. 7, pp. 1459-1476, 2005.
- [40] Yan Huang, Qining Wang, Guangming Xie, et al. "Optimal mass distribution for a passive dynamic biped with upper body considering speed, efficiency and stability. " *Humanoid Robots, 2008. Humanoids 2008. 8th IEEE-RAS International Conference on*, pp. 515-520, 2008.



Yao Wu He obtained his B. S. in Communication Engineering from Beijing Information Science and Technology University, Beijing, in 2012. Obtained his M. S. in Machine Manufacture and Automation from Beijing Technology and Business University, Beijing, in 2015. Currently,

he is pursuing the Ph. D. degree in Mechanical Engineering from Wuhan University, Wuhan, China. His research interests include biped robot dynamics and optimization control.



Daojin Yao He obtained his B. S. in Mechanical and Electronic Engineering from East China Jiaotong University, Nanchang, in 2012. Obtained his M. S. in Mechanical and Electronic Engineering from Wuhan University of Technology, Wuhan, in 2015. Currently, he is pursuing a Ph. D. in Mechanical Engineering from Wuhan University, Wuhan, China. His research interests include robot control, electronic circuit design, and embedded programming.



Xiaohui Xiao She received the B. S. and M. S. degrees in Mechanical Engineering from Wuhan University, Wuhan, China, in 1991 and 1998, respectively, and the Ph. D. degree in Mechanical Engineering from Huazhong University of Science and Technology, Wuhan, China, in 2005. She joined the Wuhan University, Wuhan, China, in 1998, where she is currently a Full Professor with the Mechanical Engineering Department, School of Power and Mechanical Engineering. She has published over 30 papers in the areas of mobile robots, dynamics and control, sensors and signal procession. Her current research interests include mobile robotics, high-precision positioning control, and signal processing.